THE JOURNAL OF BIOLOGICAL CHEMISTRY
Vol. 273, No. 28, Issue of July 10, pp. 17604–17609, 1998

Printed in U.S.A.

Crystal Structure and Mutational Analysis of the *Escherichia coli* Putrescine Receptor

STRUCTURAL BASIS FOR SUBSTRATE SPECIFICITY*

(Received for publication, January 16, 1998, and in revised form, March 20, 1998)

Dmitry G. Vassylyev‡§, Hideyuki Tomitori¶, Keiko Kashiwagi¶, Kosuke Morikawa‡, and Kazuei Igarashi¶‖

From the ‡Biomolecular Engineering Research Institute, 6-2-3 Furuedai, Suita, Osaka, 565-0874 and ¶Faculty of Pharmaceutical Sciences, Chiba University, 1-33 Yayoi-cho, Inage-ku, Chiba 263-8522, Japan

PotF protein is a periplasmic substrate-binding protein of the putrescine transport system in *Escherichia coli*. We have determined the crystal structure of PotF protein in complex with the substrate at 2.3-Å resolution. The PotF molecule has dimensions of 54 × 42 × 30 Å and consists of two similar globular domains. The PotF structure is reminiscent of other periplasmic receptors with a highest structural homology to another polyamine-binding protein, PotD. Putrescine is tightly bound in the deep cleft between the two domains of PotF through 12 hydrogen bonds and 36 van der Waals interactions. The comparison of the PotF structure with that of PotD provides the insight into the differences in the specificity between the two proteins. The PotF structure, in combination with the mutational analysis, revealed the residues crucial for putrescine binding (Trp-37, Ser-85, Glu-185, Trp-244, Asp-247, and Asp-278) and the importance of water molecules for putrescine recognition.

Natural polyamines (putrescine, spermidine, and spermine) are ubiquitous in almost all prokaryotic and eukaryotic cells. These small aliphatic cations are protonated at a physiological pH and, thus, in the cell they easily bind to nucleic acids. Through these interactions, polyamines are known to be involved in the biosynthesis of nucleic acids and proteins and to mediate the cell growth and proliferation (1, 2). Furthermore, spermidine was found to donate a portion of its molecule for the enzymatic biosynthesis of hypusine, a unique amino acid that plays a crucial role in cell proliferation (3). In the past few years, polyamines have been shown to modulate and to block a number of K^+ channels and glutamate receptors, thereby controlling the resting membrane potential and the excitability of various cells (4, 5). Studies of the factors that regulate the cellular polyamine content, therefore, are important for both basic science and medicine.

The intracellular polyamine content is controlled through the polyamine metabolism and by the uptake/excretion activities of polyamine transport systems in a concerted manner. Thus, the inhibitors of both pathways would be the potential drugs in the therapy of cancer in which the polyamines play a pathogenic role (6). Although the mechanisms of polyamine biosynthesis/degradation have been extensively studied at the molecular level, little is known about polyamine transport. No genes responsible for the transport of polyamines in mammalian cells have been isolated (6). However, three polyamine transport systems in *Escherichia coli* were recently characterized (7). One of these systems possesses putrescine uptake and excretion activities and consists of one transmembrane protein, PotE (8). The other two consist of four proteins each and have only the uptake activity, with specificity to the different polyamines. The PotA, PotB, PotC, and PotD proteins constitute the spermidine/putrescine transport system, with strong preference to spermidine (9, 10), whereas the PotF, PotG, PotH, and PotI proteins belong to the putrescine-specific transport machinery (11). In these two systems, PotF (PotD) is the primary putrescine (spermidine/putrescine) receptor in the periplasmic space. PotH and PotI (PotB, PotC) are the transmembrane components, which form the channel for the polyamines in the membrane. PotG (PotA) is the membrane-associated, ATP-binding protein that provides the energy for polyamine uptake.

PotF (PotD) belongs to the family of periplasmic binding proteins involved in active transport and chemotaxis in Gram-negative bacteria (12). A dozen high resolution x-ray structures of periplasmic receptors, with specificity to carbohydrates (13–20), sulfate (21), phosphate (22), different amino acids (23–29), and di- and oligopeptides (30, 31), have been determined in the past few years. Despite the lack of significant sequence homology, all of these proteins share a similar fold and structural topology. They consist of two globular domains with a narrow interdomain groove, which constitutes the substrate binding site. Recently, the periplasmic receptors were classified in two groups, on the basis of their three-dimensional structures. The group I proteins have three interdomain linker segments, whereas the group II proteins have only two (12).

The crystal structure of the PotD protein, which has high affinity to spermidine (K_d = 3.2 μM) and lower affinity to putrescine (K_d = 100 μM), was solved in complex with spermidine (32, 33). The atomic model and the mutational analysis (34) of the protein residues in the vicinity of the substrate binding site revealed the mechanism of spermidine recognition by the protein. However, the reason why spermidine and putrescine bind to PotD with different affinities remained obscure. The PotF and PotD proteins have 35% homology in their amino acid sequences. In addition, most of the residues involved in spermidine recognition by the PotD protein are conserved between the two proteins. Nevertheless, the PotF protein possesses a high binding affinity to only putrescine (K_d = 2.0 μM) and does not bind other polyamines. To elucidate the mechanism of substrate binding and specificity of the PotF

* The costs of publication of this article were defrayed in part by the payment of page charges. This article must therefore be hereby marked "*advertisement*" in accordance with 18 U.S.C. Section 1734 solely to indicate this fact.

§ To whom correspondence may be addressed: International Institute for Advanced Research, Matsushita Electric Industrial Co., Ltd., 3-4 Hikaridai, Seika, Soraku, Kyoto, 619-0222, Japan. Tel.: 81-774-98-2543; Fax: 81-774-98-2575.

‖ To whom correspondence may be addressed. Tel.: 81-43-290-2897; Fax: 81-43-290-2900.

TABLE I
Summary of PotF structure determination

Data collection	Native	K_2PtCl_4	K_2PtCl_4	HgI_4	HgI_4
		20 °C	*4 °C*	*2 mM*	*0.5 mM*
Resolution (Å)	50.0–2.3	50.0–3.0	50.0–3.0	50.0–3.0	50.0–3.0
Reflections					
Total (*n*)	273045	118762	136580	130340	122153
Unique (*n*)	87495	40308	40646	41073	40967
R_{sym} [a] (%)	6.9	9.0	6.7	8.7	7.6
Completeness (%)	94.0	94.0	95.0	96.0	95.8
Derivatives					
R_{iso} [b] (%)		17.6	12.6	16.3	8.5
Phasing power[c]		1.23	1.24	1.24	1.23

Refinement statistics	Native	Stereochemistry	
Resolution (Å)	10.0–2.2[d]	r.m.s.d. bond length (Å)	0.01
Number of reflections	90790	r.m.s.d. bond angles (°)	1.49
R_{cryst} [e] (%)	19.2	r.m.s.d. improper angles (°)	1.29
R_{free} [e] (%)	26.0		
Number of protein atoms	10700		
Number of water molecules	600		
Number of putrescine atoms	24		

[a] $R_{sym} = \Sigma_{hkl}\Sigma_j|I_j(hkl) - \langle I(hkl)\rangle|/\Sigma_{hkl}\Sigma_j \langle I(hkl)\rangle$, where $I_j(hkl)$ and $\langle I(hkl)\rangle$ are the intensity of measurement j and the mean intensity for the reflection with indices hkl, respectively.

[b] $R_{iso} = \Sigma_{hkl}||F_{der}(hkl)| - |F_{nati}(hkl)||/\Sigma_{hkl}|F_{nati}(hkl)|$, where $F_{der}(hkl)$ and $F_{nati}(hkl)$ are the structure factors of the heavy atom derivative and the native for the reflections with indices hkl, respectively.

[c] Phasing power = $\langle F_h\rangle/E$, where $\langle F_h\rangle$ is the root mean square heavy atom structure factor, and E is the residual lack of closure error.

[d] Although the completeness of data between 2.3- and 2.2-Å resolution was rather low (<50%), these reflections were included in the refinement to improve the ratio of number of observations to the number of refined parameters.

[e] $R_{cryst,free} = \Sigma_{hkl}||F_{calc}(hkl)| - |F_{obs}(hkl)||/\Sigma_{hkl}|F_{obs}|$, where the crystallographic R-factor is calculated including and excluding refinement reflections. The free reflections constituted 5% of the total number of reflections.

TABLE II
Oligonucleotides used for the site-directed mutagenesis of the potF gene
The mutated nucleotides are underlined.

For Sculptor™ *in vitro* mutagenesis system	
W37L	5′-GATATAATCAGACAAGTTATAAATGTG-3′
S38A	5′-GGCGATATAATCAGCCCAGTTATAAAT-3′
D39N	5′-GCGATATAATTAGACCAGTTAT-3′
Y40A	5′-GTCCGGGGCGATAGCATCAGACCAGTT-3′
S85A	5′-CAGAAAGCTGGCAGCTGGAACCACCAG-3′
S226A	5′-AATGTATTGAGATGCATGGAAATAACG-3′
W244L	5′-GACATCACCTGGCAAGCCGATAGCGAC-3′
D247A	5′-CGCCTGCCAGACAGCACCTGCCCAGCC-3′
D278N	5′-GCGAATACATTAAATAACGCC-3′
Y314A	5′-ATTGGCGTTGGCAGCGAACACATGGTC-3′
K349Q	5′-CGGATCCTGCACTTGCAGAGTGAACAG-3′
For QuikChange™ site-directed mutagenesis kit	
S87A-a	5′-GCGCTCCAGAAAGGCGGCAGATGGAAC-3′
S87A-b	5′-GTTCCATCTGCCGCCTTTCTGGAGCGC-3′
E185Q-a	5′-GGTAGCAAAAACTTGTTCTGGCGCATC-3′
E185Q-b	5′-GATGCGCCAGAACAAGTTTTTGCTACC-3′
F276L-a	5′-GAATACATCAAACAACGCCATCGCCCC-3′
F276L-b	5′-GGGGCGATGGCGTTGTTTGATGTATTC-3′

protein, we have determined the crystal structure of PotF in complex with putrescine at a 2.3-Å resolution. The mutational analysis of PotF combined with the comparison of the PotF and PotD structures provides the insight into the mechanism by which the PotF protein discriminates between the closely related putrescine and spermidine molecules.

MATERIALS AND METHODS

Bacterial Strains, Plasmids, and Culture Conditions—The spermidine uptake- and polyamine biosynthesis-deficient mutant *E. coli* KK313 (7) and its putrescine uptake-deficient mutant KK313*potF::Km* (11) were grown in medium A in the absence of polyamines as described previously (35). Plasmids pPT79 (containing the *potFGHI* genes), pPT104 (containing the *potABCD* genes), pPT79.3 (containing the *potGHI* genes), and pUC*potF* were prepared as described previously (7, 11). Plasmid pMW*potF* was prepared by inserting the 1.7-kilobase *Eco*RI-*Hin*dIII fragment of pUC*potF* into the same restriction site of pMW119 (36). Transformation of *E. coli* cells with plasmids was carried out according to the method of Maniatis *et al.* (37). Appropriate antibiotics (30 μg/ml chloramphenicol, 100 μg/ml ampicillin, and 50 μg/ml kanamycin) were added during the culture of *E. coli*.

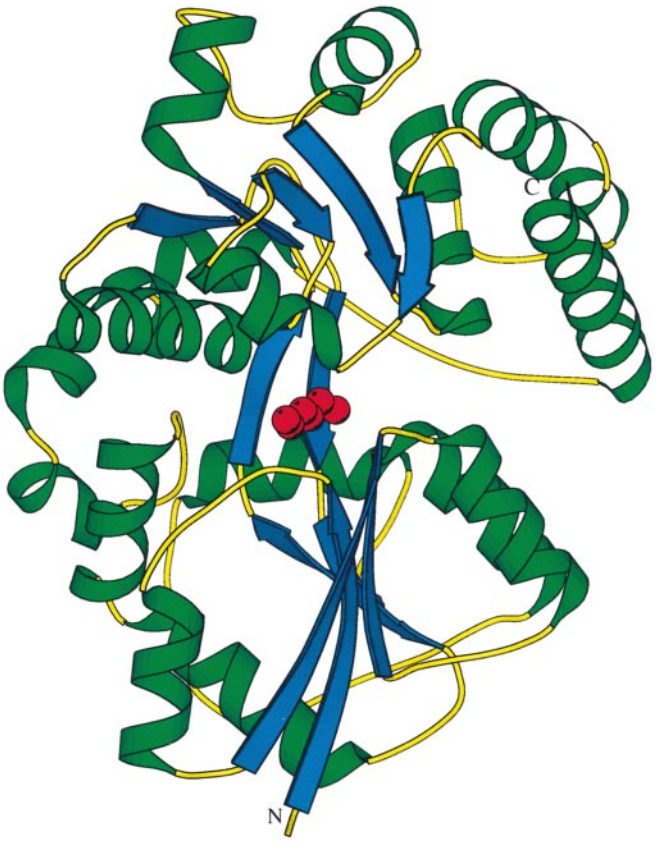

FIG. 1. **Overall view of PotF in complex with putrescine.** The PotF molecule is shown as a ribbon diagram. The β-strands, α-helices, and loop regions are *blue*, *green*, and *yellow*, respectively. The putrescine atoms are shown as *red spheres*. The figure was produced with the MOLSCRIPT program (55).

Structure Determination—PotF was crystallized, and two Pt derivatives were prepared as described previously (38). The PotF crystals belong to the space group $P2_12_12$, with unit cell dimensions a = 269.4 Å, b = 82.33 Å, and c = 93.74 Å. There are four PotF molecules in the asymmetric unit. Attempts to solve the PotF structure using molecular replacement and the PotD molecule as a search model failed. The PotF structure was solved by the multiple isomorphous replacement method, in combination with 4-fold noncrystallographic symmetry averaging (see Table I). Two crystals of the HgI_4 derivative were prepared by soaking native crystals for 2 and 4 days in solutions containing 2 mM and 0.5 mM HgI_4, respectively. The heavy atom sites for all four derivatives were refined with the MLPHARE program (39).[1] The final figure of merit at 3-Å resolution was 0.64. The multiple isomorphous replacement electron density map was improved by solvent flattening, and a rough partial poly(A)LA model was built for each of the four molecules in the asymmetric unit using the O program (40). This partial model provided an initial matrix for the noncrystallographic symmetry-related PotF molecules. The noncrystallographic symmetry averaging, in combination with solvent flattening and histogram matching (1000 cycles), was applied using the DM program (41). Almost all of the side chains and the main chain oxygens were clearly seen in the final electron density map. The atomic model was easily built in this map for one PotF molecule, using the O program (40).

Refinement—The PotF structure was refined using the slow cooling protocol in X-PLOR (42) with the manual rebuilding of the model after each refinement step (Table I). The refinement converged to an R-fac-

[1] This program was modified by D. G. Vassylyev.

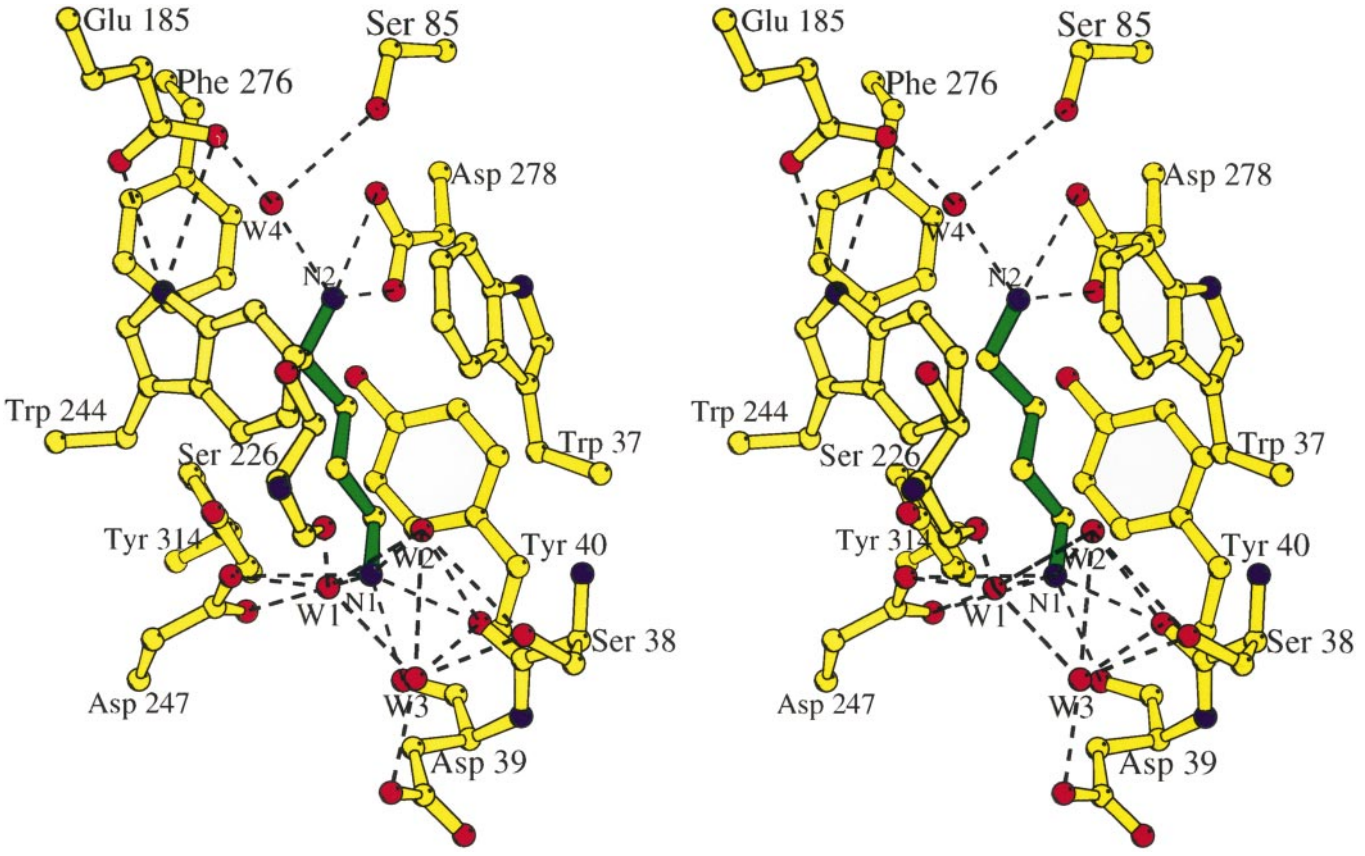

FIG. 2. **Stereo view of the PotF binding site.** Putrescine and the PotF residues involved in putrescine binding are shown as a *ball* and *stick* model. The bonds between the atoms are shown as *yellow* and *green* sticks for the PotF residues and putrescine, respectively. The atoms are drawn as the *small spheres* with atom dependent-colors (*yellow*, *blue*, and *red* for carbons, nitrogens, and oxygens, respectively). The hydrogen bonds are shown as *black dashed lines*. The figure was prepared using the MOLSCRIPT program (55).

tor = 19.2% (R-free = 26.0%). The final (2Fo-Fc) map was of high quality, with clear electron densities for the putrescine molecules bound to each of the four PotF molecules. The average B-factor was 38-Å^2 for all the protein atoms.

Mutagenesis of the PotF Gene—To prepare *potF* mutants, the 1.7-kilobase *Eco*RI-*Hin*dIII fragment of pUC*potF* was inserted into the same site of M13mp19 (43). Site-directed mutagenesis was carried out by the method of Sayers *et al.* (44) with the Sculptor™ *in vitro* mutagenesis system (Amersham Pharmacia Biotech). The mutated DNA fragments were isolated from the replicative form of M13 and were religated into the same site of pUC*potF*. Some mutants were prepared using the polymerase chain reaction (45) with the QuikChange™ site-directed mutagenesis kit (Stratagene). Mutations were confirmed by DNA sequencing (46) with commercial and synthesized primers. The sequences of the oligonucleotides used for the mutagenesis are shown in Table II.

Assay for Putrescine Binding to the PotF Protein—Periplasmic proteins were obtained from *E. coli* JM105 (*supE endA sbcB15 hsdR rpsL thi* Δ(*lac-proAB*)) (47) containing either pUC*potF* or pUC mutated *potF*, according to the method of Oliver and Beckwith (48). The PotF protein represented approximately 50% of the total periplasmic protein content, and this was used as the PotF protein source (see Fig. 3*A*). The reaction mixture (0.1 ml) containing 10 mM Tris-HCl (pH 7.5), 30 mM KCl, 10 μg of PotF protein, and 4 μM [^{14}C]putrescine (2.24 GBq/mmol) was incubated at 30 °C for 5 min. The PotF protein was collected on membrane filters (cellulose nitrate, 0.45 μm; Advantec Toyo), and the radioactivity was counted with a liquid scintillation spectrometer. The protein content was measured by the method of Lowry *et al.* (49).

Putrescine Uptake by Intact Cells—*E. coli* KK313*potF*::K_m containing pPT79.3 and pMW*potF* (or pMW mutated *potF*) was grown in medium A until the A_{540} reached 0.3. The assay for putrescine uptake was performed as described previously (50) using 10 μM [^{14}C]putrescine (370 MBq/mmol) as the substrate.

RESULTS

Structure Description—PotF consists of 370 amino acids (41 kDa), including a 26-amino acid signal peptide, which is cleaved after biosynthesis and was not included in the sample used for crystallization. The PotF crystal structure lacks three amino acids, two N-terminal and one C-terminal, which are disordered in the crystal. The PotF molecule has an ellipsoidal shape, with approximate dimensions of 54 × 42 × 30 Å, and belongs to the α/β type of proteins. It consists of two structurally similar globular domains. Each domain is composed of a central, five-stranded mixed β-sheet flanked on both sides by six and eight α-helices in the N- and C-domains, respectively (Fig. 1). Both domains consist of two distinct amino acid segments. Residues 29–133 and 279–332 constitute the N-terminal domain, whereas residues 139–273 and 347–369 form the C-terminal domain. Thus, PotF has three interdomain linker segments and belongs to group I of the periplasmic receptors according to the classification (12). Linkers 1 (residues 134–138) and 2 (residues 274–278) form a two-stranded antiparallel β-sheet at the center of the molecule, which makes up the floor of the interdomain cleft. Linker 3 (residues 333–346) is located on the molecular surface and consists of two α-helices joined by a short loop. One disulfide bridge is formed between Cys-175 and Cys-239, which stabilizes the conformation of the C-domain.

There are four PotF molecules (r.m.s.d.[2] = 0.72 Å between all of the atoms of the monomers) in the asymmetric unit of the crystal, which are arranged as a pair of dimers. Surprisingly, the noncrystallographic symmetry, which connects the molecules within the dimer, is substantially different between the two dimers. Thus, although the dimer formation involves the same protein segments in both dimers, the hydrogen bond network is considerably different.

[2] The abbreviation used is: r.m.s.d., root mean square deviation.

Putrescine Binding Site—The putrescine binding site is located in the deep cleft (26 × 6 × 10 Å) at the interface between the two PotF domains. The putrescine is almost completely engulfed in the cleft and makes multiple polar and van der Waals interactions with the PotF residues (Fig. 2). The PotF residues from both domains are involved in putrescine binding. Two putrescine amino groups are recognized through hydrogen bonds with adjacent acidic residues and main chain carbonyl oxygens. In total, there are six direct and six water-mediated hydrogen bonds between the putrescine amino nitrogens and the PotF residues. The N1 putrescine atom at the entrance of the binding cavity is hydrogen bonded to Ser-38, Asp-39, and Asp-247 and interacts with Ser-38, Asp-247, and Ser-226 through the triad of water molecules, which is conserved in all four PotF molecules (Fig. 2). The N2 atom of putrescine is completely buried in the cleft and makes strong hydrogen bonds with the carboxyl oxygens of Asp-278 and with a water molecule (W4, Fig. 2), which in turn is tightly bound to the adjacent Ser-85 and Glu-185. This water molecule (average B-factor = 30 $Å^2$) is conserved among the four independent PotF. The affinity of PotF to putrescine is enhanced through the 36 nonspecific van der Waals interactions between the putrescine atoms and the five hydrophobic PotF residues (Fig. 2). The putrescine backbone lies inside the hydrophobic cylinder, with an approximate radius of 3.6 Å formed by the PotF side chains of Trp-37, Tyr-40, and Tyr-314 from the N-domain, Trp-244 from the C-domain, and Phe-276 in the linker region.

Mutational Analysis—The crystal structure of the PotF protein in complex with putrescine revealed the protein residues involved in putrescine binding. To elucidate the functional roles of these residues in putrescine binding, mutant proteins were prepared by site-directed mutagenesis, and their putrescine affinities and uptake activities were measured (Fig. 3). Among the mutated residues, 13 corresponded to those of the spermidine binding site in the homologous PotD protein, whereas Asp-247 lacked an analogue in PotD (Fig. 4).

Putrescine binding to the mutated PotF protein was measured using 4 μM putrescine as the substrate and the periplasmic fraction prepared from *E. coli* JM105/pUC-mutated *potF*. The normal and mutated PotF represented about 50% of the total periplasmic protein (Fig. 3*A*). The putrescine binding activity was greatly decreased with the mutated PotF proteins W37L[3], D278N, W244L, and D247A in which closely located hydrophobic amino acids or acidic residues interacting with the amino groups of the putrescine are modified. The binding affinity for putrescine was also substantially decreased in the PotF mutants S38A, Y40A, Y314A, S87A, and F276L (Figs. 3*B* and 4*A*). Interestingly, the E185Q and S85A mutations significantly impaired putrescine binding to PotF. These amino acids correspond to Glu-171 and Ser-83 of the PotD protein (Fig. 4*B*) and make hydrogen bonds with the primary amine of the spermidine aminopropyl moiety, but they lack direct contacts with putrescine in the PotF binding site.

The PotF binding activity results were further confirmed by experiments with the putrescine uptake activities of intact cells containing the mutated protein. The putrescine uptake activities were measured with *E. coli* KK313*potF::Km* containing pPT79.3 and pMW-mutated *potF*. In this strain, the activity of the PotF protein is thought to be rate-limiting, because the copy number of the plasmid pPT79.3 is much higher than that of the pMW mutated *potF*. The putrescine uptake activity was greatly diminished in the PotF mutants W37L, D278N, W244L, D247A, E185Q, and S85A (Fig. 3*C*). The activity was also decreased in the mutated PotF proteins S38A, Y40A, Y314A, and S87A.

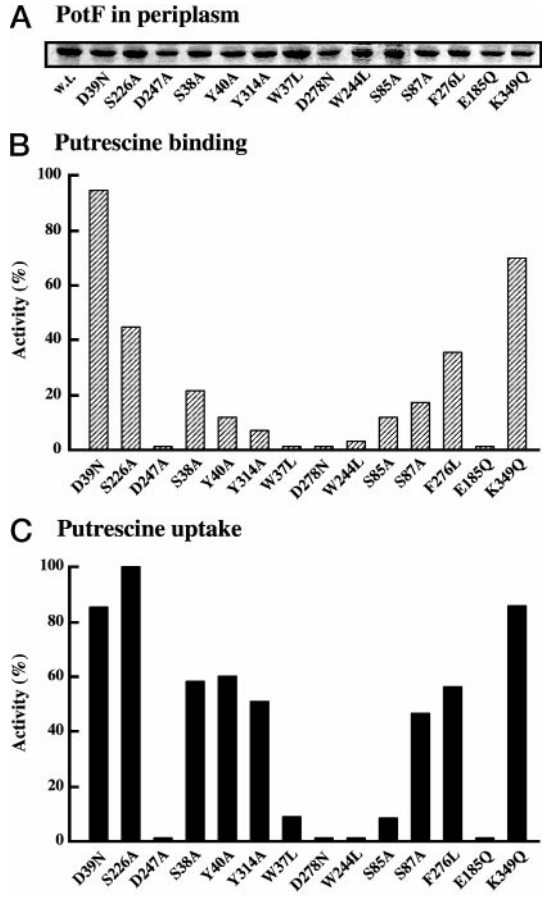

FIG. 3. **Putrescine binding and uptake activities of mutated PotF proteins.** *A*, PotF protein in periplasm. Periplasmic protein (10 μg) was electrophoresed on 12% polyacrylamide gel (56) and stained with Coomassie Brilliant Blue R250. *B*, putrescine binding. The control activity with the normal PotF protein was 3.59 nmol/mg of protein. *C*, putrescine uptake activity. The control activity was 0.66 nmol/min/mg of protein. Each value is the average of duplicate determinations.

DISCUSSION

Comparison of PotF with PotD and Other Periplasmic-binding Proteins—The two domain architecture and the topology of each domain of PotF resemble the structures of other periplasmic receptors (12). Among these, the PotF structure was most similar to its closest homologue, PotD (35% sequence identity), which in turn was shown to be similar to the maltodextrin-binding protein in the ligand-bound form (32). The r.m.s.d. between all C_α atoms of PotF and PotD was only 1.5 Å (Fig. 5). At the same time the N-domains of the two proteins exhibited better structural homology (r.m.s.d. = 1.1 Å) than their C-domains (r.m.s.d. =1.7 Å), as was also found in other periplasmic binding proteins. In contrast to PotD, PotF contains one disulfide bridge, formed between Cys-175 and Cys-239. These two cysteines are located at the beginning of two adjacent β-strands in the central β-pleated sheet of the C-domain and thus may stabilize the conformation of this β-sheet.

Substrate binding by periplasmic receptors is accompanied by the structural transition of the protein from the "open" ligand-free form to the "closed" ligand-bound conformation. The soaking of leucine into crystals of a ligand-free leucine-isoleucine-valine-binding protein has shown the presence of ligand-bound open form in which the substrate is bound to only one domain of the receptor (23). The crystal structures of some other substrate-bound periplasmic proteins revealed that, in

[3] The mutated PotF protein W37L contains leucine instead of tryptophan at position 37 from the initiator methionine.

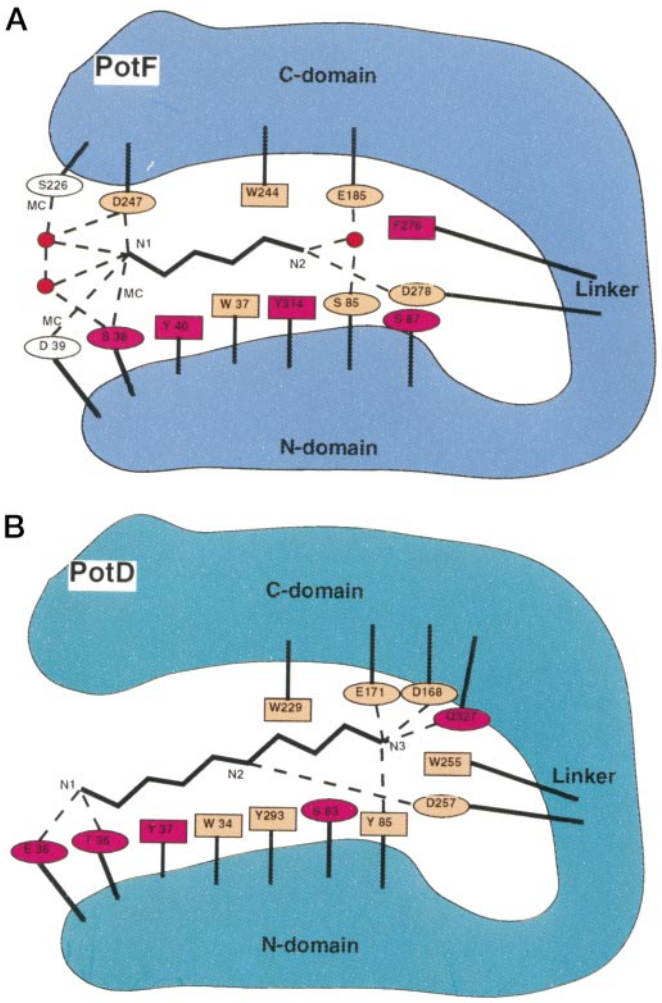

FIG. 4. **Schematic drawing of the PotF and PotD binding sites.** The polar and hydrophobic residues are drawn as *ellipses* and *rectangles*, respectively. The most crucial residues from the structural and mutational analyses are *brown*. The other residues, which should affect substrate binding according to the structural and/or mutational results, are colored *pink* or *white*. The polar interactions between proteins and substrates are shown as *black dashed lines*. *A,* putrescine binding to PotF Ser-226 and Asp-39 are shown in *white*, as their mutations did not strongly affect putrescine binding to PotF. The water molecules are shown as *red circle.* MC, main chain. *B,* spermidine binding to PotD.

FIG. 5. **Comparison of PotF and PotD.** The PotD molecule (*green*) is superimposed on the PotF molecule (*red*). Putrescine bound to PotF and spermidine bound to PotD are shown as *cyan* and *yellow ball* and *stick* models, respectively. The figure was drawn with the MOLSCRIPT program (55).

general, one domain of the receptor donates more residues for the binding of ligand than the other (17, 26, 32, 51). Thus, it is now believed that the substrates first bind to one domain of the open receptor and then stabilize the closed conformation through the interactions with the other domain. In the case of PotF, five residues of the N-domain (Trp-37, Ser-38, Asp-39, Tyr-40, and Tyr-314) are involved in putrescine binding, whereas only two residues from the C-domain (Trp-244 and Asp-247) interact with the substrate (Fig. 4*A*). Thus, it is likely that putrescine binds first to the N-domain, whereas PotF has the open conformation. There are two additional residues (Phe-276 and Asp-278) important for putrescine binding (Figs. 2 and 3), which belong to the hinge region between the two domains. The main chain torsion angle rotations of the residues in the linker regions are believed to be the major factor mediating the hinge motion between the open and closed forms in the periplasmic receptors (12). Thus, it is possible that in PotF, the initial contacts of putrescine with Phe-276 and Asp-278 would induce the transformation of the protein from the open to the closed conformation.

Polyamine Binding by PotF and PotD—PotD can bind not only spermidine but also putrescine with lower affinity. After superposition of the PotF and PotD molecules, the putrescine bound to PotF coincides well with the diaminobutane moiety of the spermidine bound to PotD (Fig. 5). Among the 13 amino acid residues that were shown to be important for spermidine binding by PotD (Fig. 4*B*), seven residues (Trp-37, Tyr-40, Ser-85, Glu-185, Trp-244, Asp-278, and Tyr-314) are absolutely conserved in the PotF sequence, and their side chains overlap well in the three-dimensional structures (r.m.s.d. = 0.8 Å). All of these residues are crucial for the putrescine binding and uptake activities of PotF (Figs. 3 and 4*A*). Surprisingly, the mutations of Ser-85 and Glu-185, which do not directly contact with putrescine, substantially impaired the PotF activities. On the other hand, they interact with the putrescine amino group through the water molecule W4 (Fig. 2 and 4*A*). The presence of this water molecule is important as it makes a barrier for putrescine in the binding cleft. The displacement of the water W4 would facilitate the penetration of putrescine deeper into the cleft and would disturb the interactions of the substrate with the major amino acid residues involved in putrescine recognition. One feasible role of Ser-85 and Glu-185 is to fix the position of the water W4, and thus, to stabilize the volume and the shape of the binding cavity. The carboxyl oxygens of Glu-185 form strong hydrogen bonds (3.0 and 3.6 Å) with the $N_{\epsilon 1}$ atom of Trp-244, which stacks on the substrate. Therefore, a second possible role of Glu-185 is to maintain the favorable orientation of the Trp-244 side chain. Among 36 van der Waals contacts between putrescine and the PotF aromatic side chains, 21 interactions are made with Trp-37 and Trp-244, which is in good agreement with the mutational analysis (Fig. 3).

Two residues in PotD, Thr-35 and Glu-36, the side chains of which hydrogen bond to the amino nitrogen N1 of spermidine

(Fig. 4*B*), are replaced by Ser-38 and Asp-39 in PotF, respectively. In contrast to PotD, putrescine hydrogen bonds not with the side chains of Ser-38 and Asp-39 but with the main chain carbonyl oxygens of these two residues (Fig. 2 and 4*A*). The side chain of Ser-38 interacts with the N1 atom of putrescine through the water molecule, W2, which explains the appreciable loss of the activity by the PotF mutant S38A (Fig. 3). Moreover, in PotF, the carboxyl oxygens of Asp-247 make two strong direct (2.8 Å, 3.5 Å) and one water-mediated (*W1*, Fig. 2) hydrogen bonds with the N1 atom of putrescine. The binding of putrescine by PotF at the N1 amino group is additionally stabilized by the water-mediated (*W1*, Fig. 2) hydrogen bond with the carbonyl oxygen of Ser-226. Thus, the binding at the N1 site of putrescine by PotF is much stronger than was observed in PotD with the similar atom of spermidine. In total, there are four direct and three water-mediated hydrogen bonds in PotF, in contrast to only two hydrogen bonds in PotD. This observation would explain the lower affinity (50 times) of PotD to putrescine than that of PotF, as the other interactions of the proteins with putrescine (the diaminobutane portion of spermidine) are very similar.

Implications for Substrate Specificity—Why does PotF bind only putrescine? Judging by the structure of PotD, the most logical explanation is that PotF recruits some bulky side chain that protrudes deeply into the binding cavity and prevents the spermidine binding by steric hindrance with the spermidine aminopropyl moiety. The alignment of the PotF and PotD sequences shows that the Gln-327 side chain in PotD, which is involved in binding to the amino group of the aminopropyl portion of spermidine, is replaced by the longer side chain of Lys-349. On the basis of the PotD structure, the PotF model was constructed in which Lys-349 blocks the binding of spermidine to PotF (33). However, this model disagrees with the PotF crystal structure. The structural alignment of the PotF and PotD sequences shows that the actual counterpart of Gln-327 (PotD) in PotF is Leu-348, the side chain of which is far from the binding site, due to the difference in the local conformations between PotD and PotF.

In PotF, the position of the N1 atom of putrescine is strictly fixed, whereas in PotD, the N1 atom of spermidine is more flexible, as discussed above. To understand whether this difference may prevent spermidine binding to PotF, we made a docking model of the spermidine molecule with a fixed position of its N1 amino group. There was no conformation that lacked steric hindrance with some protein residues in the PotF binding site. Thus, we presume that the substrate selectivity of PotF is primary dominated by the unique hydrogen bond network with the polyamine N1 amino group, so that polyamines larger than putrescine are not able to fit to the shape of the PotF binding cavity.

In conclusion, the crystal structures of the PotF and PotD proteins provide the first insight into the mechanism of specific binding and discrimination between different polyamines by biological macromolecules. The structural results, in combination with the mutational analysis, revealed that polyamine recognition could be achieved by the cooperation of multiple polar and hydrophobic interactions. The arrangement and the chemical properties of amino acids in the PotF (PotD) binding site may be used as a template for studies of other polyamine-binding proteins. One encouraging example is that a sequence comparison with PotD revealed the residues crucial for polyamine binding in a glutamate receptor (52–54).

Acknowledgments—We are grateful to Drs. Y. Maeda and K. Imada for the opportunity to use the x-ray facilities at the International Institute for Advanced Research (Kyoto, Japan) and for their assistance in the data collection. We thank Dr. Y. Kimura for providing us with computer facilities.

REFERENCES

1. Tabor, C. W., and Tabor, H. (1984) *Annu Rev. Biochem.* **53,** 749–790
2. Pegg, A. E. (1988) *Cancer Res.* **48,** 759–774
3. Park, M. H., Wolff, E. C., and Folk, J. E. (1993) *Trends Biochem. Sci.* **18,** 475–479
4. Johnson, T. D. (1996) *Trends Pharmacol. Sci.* **17,** 22–27
5. Williams, K. (1997) *Biochem. J.* **325,** 289–297
6. Seiler, N., Delcros, J. G., and Moulinoux, J. P. (1996) *Int. J. Biochem. Cell Biol.* **28,** 843–861
7. Kashiwagi, K., Hosokawa, N., Furuchi, T., Kobayashi, H., Sasakawa, C., Yoshikawa, M., and Igarashi, K. (1990) *J. Biol. Chem.* **265,** 20893–20897
8. Kashiwagi, K., Shibuya, S., Tomitori, H., Kuraishi, A., and Igarashi, K. (1997) *J. Biol. Chem.* **272,** 6318–6323
9. Furuchi, T., Kashiwagi, K., Kobayashi, H., and Igarashi, K. (1991) *J. Biol. Chem.* **266,** 20928–20933
10. Kashiwagi, K., Miyamoto, S., Nukui, E., Kobayashi, H., and Igarashi, K. (1993) *J. Biol. Chem.* **268,** 19358–19363
11. Pistocchi, R., Kashiwagi, K., Miyamoto, S., Nukui, E., Sadakata, Y., Kobayashi, H., and Igarashi, K. (1993) *J. Biol. Chem.* **268,** 146–152
12. Quiocho, F. A., and Ledvina, P. S. (1996) *Mol. Microbiol.* **20,** 17–25
13. Quiocho, F. A., and Vyas, N. K. (1984) *Nature* **310,** 381–386
14. Quiocho, F. A., Wilson, D. K., and Vyas, N. K. (1989) *Nature* **340,** 404–407
15. Vyas, N. K., Vyas, M. N., and Quiocho, F. A. (1988) *Science* **242,** 1290–1295
16. Vyas, M. N., Vyas, N. K., and Quiocho, F. A. (1994) *Biochemistry* **33,** 4762–4768
17. Zou, J., Flocco, M. M., and Mowbray, S. L. (1993) *J. Mol. Biol.* **233,** 739–752
18. Flocco, M. M., and Mowbray, S. L. (1994) *J. Biol. Chem.* **269,** 8931–8936
19. Quiocho, F. A., Spurlino, J. C., and Rodseth, L. E. (1997) *Structure* **5,** 997–1015
20. Mowbray, S. L., and Cole, L. B. (1992) *J. Mol. Biol.* **225,** 155–175
21. Pflugrath, J. W., and Quiocho, F. A. (1985) *Nature* **314,** 257–260
22. Luecke, H., and Quiocho, F. A. (1990) *Nature* **347,** 402–406
23. Sack, J. S., Saper, M. A, and Quiocho, F. A. (1989) *J. Mol. Biol.* **206,** 171–191
24. Sack, J. S., Trakhanov, S., Tsigannik, I. H., and Quiocho, F. A. (1989) *J. Mol. Biol.* **206,** 193–207
25. Kang, C.-H., Shin, W.-C., Yamagata, Y., Gokcen, S., Ames, G. F.-L., Kim, S.-H. (1991) *J. Biol. Chem.* **266,** 23893–23899
26. Oh, B., Pandit, J., Kang, C.-H., Nikaido, K., Gokcen, S., Ames, G. F.-L., and Kim, S.-H. (1993) *J. Biol. Chem.* **268,** 11348–11355
27. Oh, B., Kang, C.-H., De Bondt, H., Kim, S.-H., Nikaido, K., Jashi, A. K., and Ames, G. F.-L. (1994) *J. Biol. Chem.* **269,** 4135–4143
28. Yao, N., Trakhanov, S., and Quiocho, F. A. (1994) *Biochemistry* **33,** 4769–4779
29. Hsiao, C.-D., Sun, Y.-J., Rose, J., and Wang, B.-C. (1996) *J. Mol. Biol.* **262,** 225–242
30. Nickitenko, A. V., Trakhanov, S., and Quiocho, F. A. (1995) *Biochemistry* **34,** 16585–16595
31. Tame, J. R. H., Murshudov, G. N., Dodson, E. J., Neil, T. K., Dodson, G. G., Higgins, C. F., and Wilkinson, A. J. (1994) *Science* **264,** 1578–1581
32. Sugiyama, S., Vassylyev, D. G., Matsushima, M., Kashiwagi, K., Igarashi, K., and Morikawa, K. (1996) *J. Biol. Chem.* **271,** 9519–9525
33. Sugiyama, S., Matsuo, Y., Maenaka, K., Vassylyev, D. G., Matsushima, M., Kashiwagi, K., Igarashi, K., and Morikawa, K. (1996) *Protein Sci.* **5,** 1984–1990
34. Kashiwagi, K., Pistocchi, R., Shibuya, S., Sugiyama, S., Morikawa, K., and Igarashi, K. (1996) *J. Biol. Chem.* **271,** 12205–12208
35. Kashiwagi, K., Yamaguchi, Y., Sakai, Y., Kobayashi, H., and Igarashi, K. (1990) *J. Biol. Chem.* **265,** 8387–8391
36. Yamaguchi, K., and Masamune, Y. (1985) *Mol. Gen. Genet.* **200,** 362–367
37. Maniatis, T., Fritsch, E. F., and Sambrook, J. (1982) *Molecular Cloning: A Laboratory Manual,* pp. 250–251, Cold Spring Harbor Laboratory, Cold Spring Harbor, NY
38. Vassylyev, D. G., Kashiwagi, T., Tomitori, H., Kashiwagi, K., Igarashi, K., and Morikawa, K. (1998) *Acta Crystallogr. Sec. D* **54,** 132–134
39. Otwinowski, Z. (1991) in *Proceedings of CCP4 Study Weekend, 25–26 January 1991* (Wolf, W., Evans, P. R., and Leslie, A. G. W., eds) pp. 80–86, Daresbury Laboratory, Warrington, United Kingdom
40. Jones, T. A., Zou, J. Y., Cowan, S. W., and Kjeldgaard, M. (1991) *Acta Crystallogr. Sec. A* **47,** 110–119
41. Collaborative Computational Project 4 (1994) *Acta Crystallogr. Sec. D* **50,** 760–763
42. Brunger, A. T. (1992) *X-PLOR*, Version 3.1 manual, Yale University Press, New Haven, Connecticut
43. Yanisch-Perron, C., Vieira, J., and Messing, J. (1985) *Gene (Amst.)* **33,** 103–119
44. Sayers, J. R., Krekel, C., and Eckstein, F. (1992) *Biotechniques* **13,** 592–596
45. Saiki, R. K., Gelfand, D. H., Stoffel, S., Scharf, S. J., Higuchi, R., Horn, J. T., Mullis, K. B., and Erlich, H. A. (1988) *Science* **239,** 487–491
46. Sanger, F., Nicklen, S, and Coulson, A. R. (1977) *Proc. Natl. Acad. Sci. U. S. A.* **74,** 5463–5467
47. Sambrook, J., Fritsch, E. F., and Maniatis, T. (1989) *Molecular Cloning: A Laboratory Manual,* pp. 10–12, Cold Spring Harbor Laboratory, Cold Spring Harbor, NY
48. Oliver, D. B., and Beckwith, J. (1982) *Cell* **30,** 311–319
49. Lowry, O. H., Rosebrough, N. J., Farr, A. L., and Randall, R. J. (1951) *J. Biol. Chem.* **193,** 265–275
50. Kashiwagi, K., Kobayashi, H., and Igarashi, K. (1986) *J. Bacteriol.* **165,** 972–977
51. Sharff, A. J., Rodseth, L. E, Spurlino, J. C., and Quiocho, F. A. (1992) *Biochemistry* **31,** 10657–10663
52. Williams, K., Kashiwagi, K., Fukuchi, J., and Igarashi, K. (1995) *Mol. Pharmacol.* **48,** 1087–1098
53. Kashiwagi, K., Fukuchi, J., Chao, J., Igarashi, K., and Williams, K. (1996) *Mol. Pharmacol.* **49,** 1131–1141
54. Kashiwagi, K., Pahk, A. J., Masuko, T., Igarashi, K., and Williams, K. (1997) *Mol. Pharmacol.* **51,** 861–871
55. Kraulis, P. J. (1991) *J. Appl. Cryst.* **24,** 946–950
56. Laemmli, U. K. (1970) *Nature* **227,** 680–685